8-16-2024

Estuarine Microbial Community Composition and Efficiency Changes in Response to Vibrio Parahaemolyticus Exposure

Sarah Mulligan
University of South Carolina

Estuarine microbial community composition and efficiency changes in response to *Vibrio parahaemolyticus* exposure

By

Sarah Ann Mulligan

Bachelor of Science
Florida Southern College, 2020

Submitted in Partial Fulfillment of the Requirements

For the Degree of Master of Science in

Biology

College of Arts and Sciences

University of South Carolina

2024

Accepted by:

James Pinckney, Director of Thesis

Tammi Richardson, Reader

Xuefeng Peng, Reader

Ann Vail, Dean of the Graduate School

Acknowledgements

This work would not have been possible without my wonderful advisor, Dr. James L Pinckney. He allowed me the freedom to explore my interests and develop my own project, which led me to work with *V. parahaemolyticus*. His love of science and phytoplankton is inspiring. He provided the perfect level of guidance and support throughout my time at the University of South Carolina.

I also want to thank my other committee members, Dr. Tammi Richardson and Dr. Xuefeng Peng, both from the University of South Carolina. They both assisted with this project and provided feedback to allow me to make this project the best it can be.

Dr. Karlen Correa Velez and Dr. Sean Norman were also extremely helpful throughout the bioassays. Karlen put in a lot of time to assist me with the *V. parahaemolyticus* work and I am very grateful for her expertise.

Finally, I would not have been able to complete this project without the support of my friends and family. They were there for me every step of the way, and I will never stop being grateful for them.

Abstract

Vibrio parahaemolyticus is a pathogenic bacterium whose full impact on natural estuarine phytoplankton communities has not been fully resolved. The primary goal of this research was to test how the addition of *V. parahaemolyticus* to a natural estuarine microbial community would impact the other microbes present. We hypothesized *V. parahaemolyticus* exposure would reduce phytoplankton biomass and alter the composition of phytoplankton and bacterial communities. Experimental bioassays (60h) were used to assess the effects of the presence of *V. parahaemolyticus*. Samples for measurements of chemotaxonomic photopigment concentrations, 16S sequencing-based community composition, photosynthetic efficiency, cell density, and *V. parahaemolyticus* abundance were collected throughout the incubation. There was a significant difference between the exposed- and nonexposed-groups for chl-*a*, indicating a decrease in overall phytoplankton biomass. ChemTax analysis also revealed there was a decrease in the relative abundances of diatoms, cryptophytes, and cyanobacteria. There was also a change in bacterial community composition, with eight phyla decreasing in relative abundance and one phyla increasing in relative abundance. These results suggest *V.*

parahaemolyticus may have a significant impact on microbial communities in estuarine ecosystems and should be closely monitored, as changes in microbial communities can result in ecological and chemical changes in habitats; in addition, the seafood industry should test for the presence of *V. parahaemolyticus* in their products, especially during the summer months when phytoplankton and bacterial populations thrive.

Table of Contents

Acknowledgements ii

Abstract iii

List of Tables vi

List of Figures vii

Chapter One: Introduction 1

Chapter Two: Methods 5

Chapter Three: Results 11

Chapter Four: Discussion 18

References 26

Appendix A: Supplemental Figures 35

Appendix B: Supplemental Methods 40

List of Tables

Table 3.1 The significant MANOVA results for changes in estimated abundances of algal groups at 60h and the sample means and standard deviations 12

Table 3.2 The significant MANOVA results for changes in relative concentrations of cells at 60h and the sample means and standard deviations 14

Table A.1 The CFU counts of *V. parahaemolyticus* at each time point 36

Table A.2 MANOVA results with sample means and standard deviations for photopigment concentrations at 60h 39

Table B.1 Seawater media components 40

List of Figures

Figure 3.1. The estimated abundance of each of the five algal classes at 60h ... 12

Figure 3.2. Relative abundance of each phylum identified during 16S sequencing ... 14

Fig. 3.3. The percent (%) difference at 60h of the average number of ASV reads of the selected prokaryotic phyla ... 16

Fig. 3.4. Relative abundance of each order identified during 16S sequencing ... 17

Figure A.1. The optical density (indicative of cell concentration) at each time point for each experimental group ... 35

Figure A.2. The quantum efficiency (F_v/F_m) of each experimental condition at 60h ... 37

Figure A.3. The concentrations of chl-*a*, zeaxanthin, peridinin, chl-*b*, alloxanthin, and fucoxanthin at 60h for both experimental conditions ... 38

Chapter One: Introduction

Vibrio parahaemolyticus is a bacterium present in marine and estuarine environments in relatively low abundances, typically less than 100,000 cells l^{-1} (Su & Liu 2007; Baker-Austin et al. 2010). Seafood contamination with *V. parahaemolyticus* is frequent and ingestion of contaminated seafood causes acute gastroenteritis, resulting in approximately 34,000 hospitalized cases of infections in the United States per year (Drake et al. 2007; Brumfield et al. 2023). Clinical isolates of *V. parahaemolyticus* contain *tlh, trh,* and/or *tdh* genes (Su & Liu 2007; Rosales et al. 2022). Only the *tdh* and *trh* genes have been proven to cause virulence (Su & Liu 2007; Matsuda et al. 2018; Brumfield et al. 2023). Strains negative for these genes still cause physical symptoms in mice, but other virulence-causing genes have not yet been identified (Su & Liu 2007).

V. parahaemolyticus has negative effects on other living organisms in the environment. T6SS1, a *V. parahaemolyticus* gene, is responsible for producing compounds harmful to other bacteria (Salomon et al. 2013). Additionally, in monocultures of eukaryotic microalgae, both virulent and nonvirulent *V. parahaemolyticus* strains decrease algal biomass (Klein et al. 2019). In these monocultures, the biomass of the coccolithophore *Emiliania huxleyi* decreased by

up to 96.3%. The biomass of the diatom *Thalassiosira pseudonana* and the dinoflagellate *Prorocentrum minimum* each decreased by up to 53.3%. Decreases in algal biomass and changes in community composition may cause upward cascading trophic effects, as phytoplankton are the base of most aquatic food webs.

The species composition of the phytoplankton community is just as important as the total abundance of phytoplankton due to the different functional purposes of each type of phytoplankton (Aiken et al. 2009; Pan et al. 2011). Different types of phytoplankton have different nutritional requirements and output different molecules and byproducts. Therefore, shifts in phytoplankton community composition, natural or not, may alter the function of the ecosystem (Heil et al. 2007; Camarena-Gomez et al. 2018). Similarly, prokaryotic organisms, such as bacteria and archaea, play a variety of roles in marine ecosystems and shifts in community composition may have ecosystem-wide impacts (Logue et al. 2016; Rath et al. 2019.

Previous experiments on the effect of *V. parahaemolyticus* on phytoplankton feature only monocultures, and the results may not be representative of the effect of *V. parahaemolyticus* on natural phytoplankton communities. Natural microbial communities are extremely diverse, especially in estuarine environments (Sun et al. 2014; Crump & Bowen 2024), and microbes impact one another in countless ways (Amin et al. 2015; Filho et al. 2021). The response of phytoplankton to *V. parahaemolyticus* in a multi-species culture with

a variety of functional groups present may be different than in a phytoplankton monoculture due to the presence of other microbes. The purpose of this research was to determine whether adding *V. parahaemolyticus* to a natural estuarine microbial community would decrease phytoplankton biomass and photosystem efficiency as well as cause a shift in community composition toward diatoms and other large phytoplankton.

Additionally, we hypothesized there would be minimal change in bacterial community composition aside from the increase in *V. parahaemolyticus*. While *V. parahaemolyticus* does impact some bacterial species when grown axenically (Salomon et al. 2013), shifts in the autotrophic community generally result in shifts in the heterotrophic community (Camarena-Gomez et al. 2018). However, it takes time for the phototrophic community to change, then time subsequentially for the heterotrophic community to change; therefore, only the direct impacts of *V. parahaemolyticus* are examined here.

V. parahaemolyticus may pose a major concern for ecosystem health. If the presence of *V. parahaemolyticus* can decrease algal biomass and productive capacity in laboratory-monitored natural community assemblages, then it may decrease algal biomass and productive capacity in estuarine and marine environments. These decreases could have detrimental impacts on food web stability and on C fixation rates in estuarine and coastal waters.

Furthermore, *V. parahaemolyticus* may increase in the coming years. The incidence of algal blooms is increasing due to eutrophication and bacterial

communities thrive in the period following an algal bloom (Main et al. 2015; Klein et al. 2019). Algal blooms can result in low oxygen concentrations, which is harmful for many organisms, but there is a large influx of C due to senescent and lysed phytoplankton cells, which heterotrophic bacteria such as *Vibrio* spp. can use to replicate rapidly. *V. parahaemolyticus* also favors warm waters of >20° C with low to moderate salinity and a pH of 5-6 (Baker-Austin et al. 2010; Correa Velez et al. 2023). As seawater temperatures rise due to climate change, this bacterium's abundance may increase and geographic range may expand. Quantifying the impact of *V. parahaemolyticus* on the microbial community is an essential first step in assessing the impact this bacterium may have on phytoplankton communities in coastal environments. This knowledge can inform important management decisions and help us keep ecosystems as healthy as possible. If *V. parahaemolyticus* has a large impact on microbial communities, it may be important for environmental managers to begin tracking the presence and concentration of *V. parahaemolyticus* in coastal waters, especially in areas where seafood is being harvested.

The purpose of our research was to take the first step towards understanding this impact and to identify the necessary next steps for research and for environmental management. We aim to quantify the impact of *V. parahaemolyticus* on estuarine phytoplankton and microbial community composition.

Chapter Two: Methods

Culturing *V. parahaemolyticus*:

A culture of the C12 strain of *V. parahaemolyticus* was obtained from the Norman Microbial Lab in the Arnold School of Public Health at the University of South Carolina. The C12 strain was isolated from Winyah Bay, South Carolina, USA originally and is nonvirulent (Correa Velez et al. 2023). Due to the fast generation time of *V. parahaemolyticus*, approximately 20 minutes, cultures were inoculated in autoclaved artificial seawater media (see Table B.1) once per day to maintain the cultures. All work with *V. parahaemolyticus* cultures was performed in a Bio-Safety Cabinet due to the bacterium's Biosafety Level Two (BSL-2) status. The cultures were grown in a vial-shaking dark incubator kept at 26° C.

Performing Bioassays:

Ten (10) sterile, transparent containers (850 ml each) were filled with seawater collected from Winyah Bay, South Carolina ([33.37 N, -79.27 W], low ebb tide, pH 6.8, salinity 0.2%). After the containers were transported back to the lab, inorganic nutrients were immediately added to each of the bottles to ensure microorganisms would have the necessary nutrients to survive. For nitrogen, $NaNO_3$ was added at a final concentration of 10 µmol N L^{-1}. For phosphate, KH_2PO_4 was added at a final concentration of 2 µmol P L^{-1}. These concentrations

were used due to the standard nutrient requirements of phytoplankton in a laboratory culture (Beardall et al. 2001). Finally, a culture of *V. parahaemolyticus* (50 ml) was pelleted in a centrifuge (5 minutes at 1,000 RPM) and washed with filtered seawater (obtained from the same sampling location, run through a 0.2 µm filter to remove almost all cells) to remove any trace elements of the seawater media. After resuspending the cells in filtered seawater, 100 µl of the inoculum was added to each of the bioassay bottles.

Immediately following inoculation, subsamples (150 ml) were taken from each of the 10 bottles then filtered onto Sterlitech GF/F (2.5 cm, 0.7 µm nominal retention) glass fiber filters to process for phytoplankton biomass and community composition based on photopigment concentrations determined by High-Performance Liquid Chromatography (HPLC). Additionally, 1 ml was taken from each bottle to measure the quantum yield of photosynthesis (F_v/F_m) using a Pulse-Amplitude Modulated (PAM) Fluorometer. Next, 100 µl was taken from each bottle to measure the optical density. Another 110 µl was taken from each bottle to plate and obtain CFU counts. Finally, 10 ml was taken from each bottle to pellet and freeze at -80° C for sequencing. The bottles were then placed in an environmental chamber at 22° C at a 12-hour light/dark cycle with an irradiance of ca. 500 µmol photons m^{-2} s^{-1}.

Every 12 hours, samples were taken for PAM, optical density, and plate counts. The assays ran for 60 hours. At the 60h sampling, 10 ml was again taken from each bottle to process for sequencing and 150 ml was taken to process for

photopigment concentration analysis. The remaining liquid was then discarded according to BSL-2 safety procedures.

Phytoplankton Community Composition:

High-performance liquid chromatography (HPLC) was used to determine chemosystematic photosynthetic pigment concentrations. A graduated cylinder was used to measure 150 ml of each sample, then a vacuum pump was used to filter each sample through a 0.7 µm glass fiber filter. Each filter was placed in a labeled microcentrifuge tube, and the samples were stored at -80° C until processing. Samples were lyophilized for 24 h at -50° C, placed in 90% acetone (1 ml) and extracted at -20° C for 18–20 h. Filtered extracts (0.45 µm, 250 µl) were injected into a Shimadzu 2050 HPLC equipped with a monomeric (Rainin Microsorb-MV, 0.46 x 10 cm, 3 µm) and a polymeric (Vydac 201TP54, 0.46 x 25 cm, 5 µm) reverse-phase C18 column in series. A nonlinear binary gradient of 80% methanol:20% 0.50 M ammonium acetate and 80% methanol:20% acetone was the mobile phase (Pinckney et al. 1996, 2001). Absorption spectra and chromatograms (440 ± 4 nm) were acquired using a Shimadzu photodiode array detector. Pigment peaks were identified by comparison of retention times and absorption spectra with pure carotenal and chlorophyll standards (DHI, Denmark). The synthetic carotenoid β-apo-8'-carotenal (Sigma) was used as an internal standard.

ChemTax (v. 1.95) was used to estimate the relative concentrations of major algal groups based on measured photopigment concentrations (Pinckney

et al. 2001; Higgins et al. 2011). Total chlorophyll a (chl-*a*) was partitioned into algal group (e.g., diatoms, cyanobacteria, cryptophytes, etc.) relative abundances. Representative accessory pigments were used to estimate these partitions; e.g., diatoms are represented by the concentration of fucoxanthin, cyanobacteria by the concentration of alloxanthin, etc. (Yentsch & Phinney 1985; Millie et al. 2002). The initial ratio matrix randomization procedure with 60 simulations was used to minimize errors in algal group biomass resulting from inaccurate pigment ratio seed values (Higgins et al. 2011).

Photosynthetic Efficiency:

A Walz Water-PAM was used to allow for the ultrasensitive chlorophyll fluorescence measurement of liquid samples. Before each sample, the PAM Fluorometer was Auto-zeroed with Milli-Q water. The sample (1 ml) was pipetted into the cuvette, placed in the PAM Fluorometer, the lid closed, and the program (Phyto-WIN) started. When analyzing the samples containing *V. parahaemolyticus*, Parafilm was placed over the cuvette to avoid contaminating the PAM Fluorometer. The program calculated the quantum efficiency (F_v/F_m), which can range from 0.0 to 0.8 and is an indicator of phytoplankton photosystem efficiency (Giannini & Ciotti 2016).

Cell Concentration:

A sample from each of the incubation containers (100 µl) was pipetted into designated wells of a 96-well plate. The plate was placed in a PerkinElmer Victor

X3 and an instantaneous reading of optical density was taken at 600 nm absorbance to estimate total cell concentration at each time point.

V. parahaemolyticus Abundance:

CHROM-agar Vibrio plates were crafted according to manufacturer instructions. During the bioassay, 110 µl of each replicate was taken every 12h. The majority of the sample (100 µl) was placed directly onto a plate as the non-diluted sample (called "D1"). A subsample (10 µl) sample was placed into 100 µl of filtered seawater, and 100 µl of this mixture was placed onto a plate ("D2"). A subsample (10 µl) of the D2 mixture was placed into another 100 µl of filtered seawater, and 100 µl of this mixture was placed onto a plate ("D3"). Finally, a subsample (10 µl) of the D3 mixture was placed into another 100 µl of filtered seawater, and 100 µl of this mixture was placed onto a plate ("D4"). These plates were placed in a dark incubator at 32° C for 12h before being enumerated using a Quebec Colony Counter.

Prokaryotic Community Composition:

Cell pellets were frozen at –80° C until DNA extraction. DNA extraction was performed using Qiagen's DNeasy Plant Mini Kit according to manufacturer instructions. DNA concentration (ng μl^{-1}) and purity (A260/A280 10 mm path) were recorded using the Nanodrop 2000c Spectrophotometer with a 340 nm baseline correction. Sequencing was performed at the University of California-

Davis's Host Microbiome Systems Biology Core on the Element Aviti platform with the PE300 kit.

On a Hyperion bash shell, Qiime2 and DADA2 were used to clean, trim, and process the sequencing results. The silva138-99-341-806-nb classifier was used to match the reads to taxonomic classifications. The code used for this process can be found here.

Chapter Three: Results

The optical density of the samples did not change significantly throughout the experiment (Multi-factor ANOVA: $F_{5,48} = 1.493$, $p = 0.210$; see Fig. A.1). The plate data confirms *V. parahaemolyticus* was present in extremely high concentrations throughout the incubation period in the WV condition; most of the plates were covered by a bacterial lawn of *V. parahaemolyticus* (see Table A.1). There was no significant difference in quantum efficiency (F_v/F_m) at 60h between the W and WV conditions (ANOVA: $F_{1,8} = 0.017$, $p = 0.900$. See Figure A.2).

There were significant differences in chl-*a*, fucoxanthin, zeaxanthin, and alloxanthin concentrations between the two groups (see Fig. A.3 and Table A.2). There was not a significant difference in peridinin or chl-*b* concentrations between the two groups. Consistent with the results of photopigment concentrations, ChemTax analysis revealed there were significantly lower estimated abundances of diatoms, cryptophytes, and cyanobacteria in the WV group than in the W group (Fig. 3.1, Table 3.1). There was no significant difference in the estimated abundances of green algae or dinoflagellates. Diatoms remained the most abundant algal group with and without the *V.*

parahaemolyticus exposure, with mean estimated abundances of 13.353533 ug chl-*a* l^{-1} and 19.535545 ug chl-*a* l^{-1}, respectively (Table 3.1).

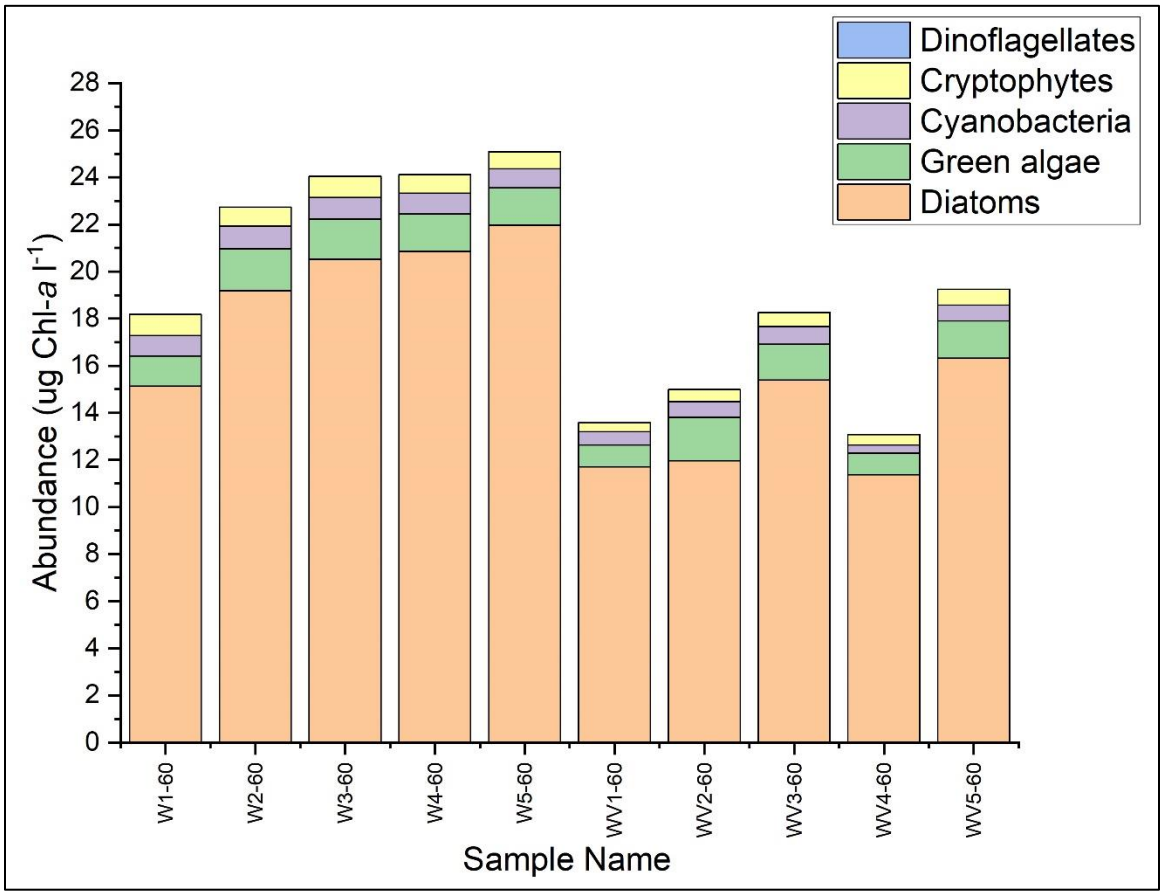

Fig 3.1. The ChemTax estimated abundance of each of the five algal classes at 60h in units of ug Chl-*a* l^{-1} for each sample displayed in a stacked bar chart.

Table 3.1. The significant MANOVA results for changes in estimated abundances of algal groups at 60h and the sample means and standard deviations

Algal group	**$F_{1,8}$**	**p-value**	**W $\bar{x}$ ± SD**	**WV $\bar{x}$ ± SD**
Diatoms	15.365	0.004*	19.535545 ± 2.6541843	13.353533 ± 2.3219985

Green algae	1.313	0.285	1.589951 ± 0.1874423	1.355389 ± 0.4176031
Cyanobacteria	14.489	0.005*	0.885423 ± 0.0628323	0.601938 ± 0.1542232
Cryptophytes	24.776	0.001*	0.820233 ± 0.0688459	0.520776 ± 0.1155739
Dinoflagellates	0.011	0.919	0.001244 ± 0.0019034	0.001417 ± 0.0031682

At 60h, there were significant decreases in the relative abundances of members of the Proteobacteria, Actinobacteriota, Planctomycetota, Verrucomicrobiota, SAR 324, Chloroflexi, Myxococcota, Fibrobacterota, Nanoarchaeota, and NB1-j phyla (Figure 3.2, Table 3.2). At 60h, there was also a significant increase in the relative abundance of members of the Dependentiae and Ochrophyta phyla. There was not a significant difference in the concentrations of the other fifty-two (52) phyla identified.

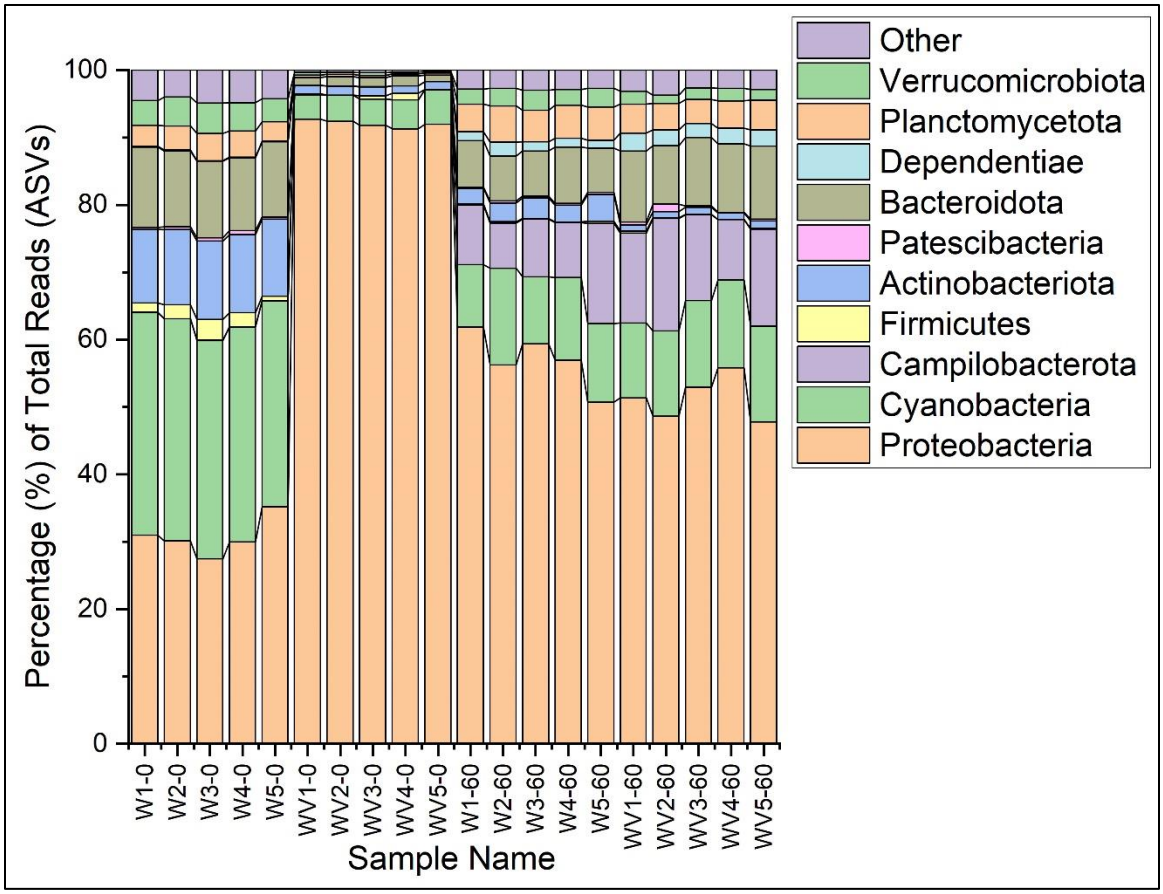

Figure 3.2. Relative abundance of each phylum identified during 16S sequencing represented by the percentage (%) of total amplicon sequence variants (ASVs) for each phylum for each replicate at 0h and 60h. The ten (10) most abundant phyla are shown while the remaining 53 phyla are grouped together as "Other."

Table 3.2. MANOVA results with sample means and standard deviations for photopigment concentrations at 60h

Phylum	**$F_{1,8}$**	**P-value**	**W $\bar{x}$ ± SD**	**WV $\bar{x}$ ± SD**
Proteobacteria	7.227	0.028	58171.8 ± 6583.499	43487.8 ± 10287.28
Actinobacteriota	34.119	< 0.001	2975.2 ± 763.54	857.4 ± 272.53

Dependentiae	6.124	0.038	1463 ± 282.39	1973.2 ± 364.41
Planctomycetota	10.587	0.012	4892.8 ± 616.65	3418.6 ± 803.8
Verrucomicrobiota	18.806	0.002	2644.2 ± 491.6	1416.6 ± 398.7
SAR 324	40.108	< 0.001	428.8 ± 63.4	195.8 ± 52.4
Chloroflexi	13.741	0.006	359.8 ± 67.2	202.8 ± 66.7
Myxococcota	11.142	0.010	288.2 ± 51.84	168.8 ± 60.91
Fibrobacterota	36.800	< 0.001	18.8 ± 6.72	0.400 ± 0.894
Nanoarchaeota	13.158	0.007	17.2 ± 8.79	2.60 ± 1.95
NB1-j	5.625	0.045	3.00 ± 2.83	0.00 ± 0.00
Ochrophyta	29.920	< 0.001	0.400 ± 0.894	15.4 ± 6.07

Fibrobacterota had the largest percent (%) change of the phyla that changed significantly with the addition of *V. parahaemolyticus* with a 100% decrease (Figure 3.3). This phylum had an extremely small average concentration at the beginning of the incubation (3.000 ASV reads).

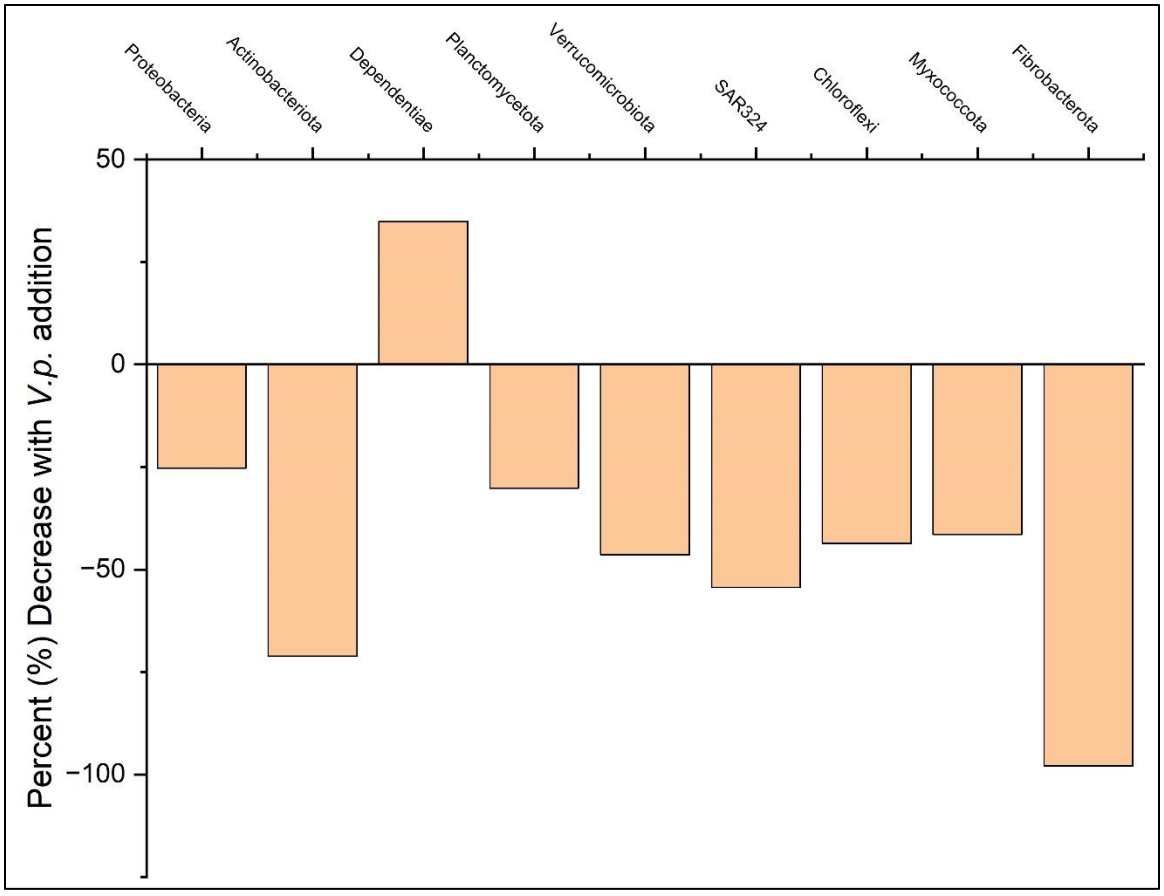

Figure 3.3. The percent (%) difference at 60h of the average number of ASV reads of the selected prokaryotic phyla between the groups without and with *V. parahaemolyticus* present.

At the Order level, there was overall no significant difference at 60h between the W and WV groups (MANOVA: $F_{1,8} = 10.711$, $p = 0.232$). Individual orders could therefore not be examined. The ten most abundant orders can be seen below (Fig. 3.4).

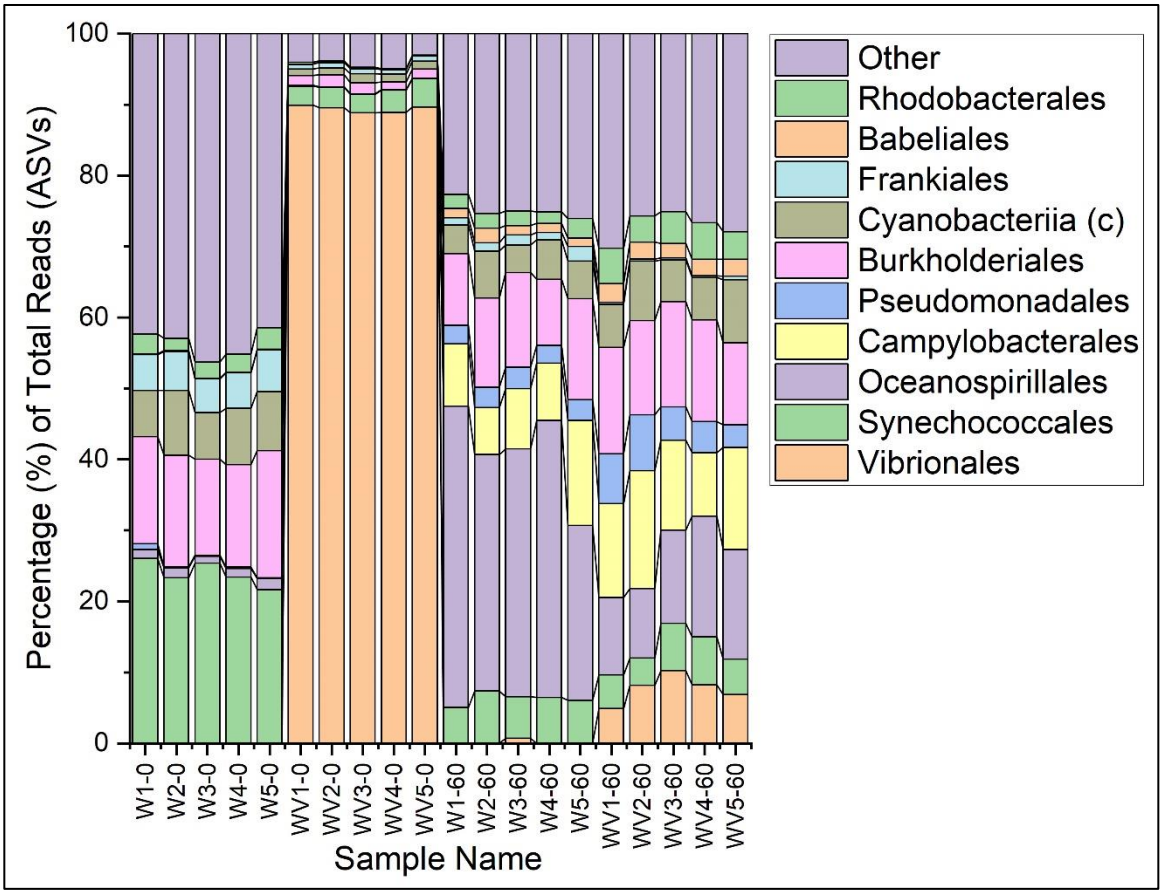

Figure 3.4. Relative abundance of each order identified during 16S sequencing represented by the percentage (%) of total amplicon sequence variants (ASVs) for each order for each replicate at 0h and 60h. The ten (10) most abundant orders are shown while the rest of the 396 orders are grouped together as "Other." Cyanobacteriia was grouped only to the class level.

Chapter Four: Discussion

The optical density data (Fig. A.1) indicates culture densities were relatively constant over the duration of the bioassay and confirms a nearly constant cell survival over the duration of the bioassay. The CHROM-agar plate data (Table A.1) shows the abundance of *V. parahaemolyticus* specifically and confirms its presence in high concentrations throughout the bioassay. In nature, *V. parahaemolyticus* can survive in low concentrations using the low ambient dissolved organic C (DOC) concentrations (Correa Velez et al. 2023). However, in the laboratory setting, there is no constant influx of phytoplankton exudates, senescent/dead or lysed cells, or alternative nutrient input to sustain high concentrations of heterotrophic bacteria. Preliminary experiments suggested *V. parahaemolyticus* would not be able to survive for an extended period in a laboratory setting without an added C source. However, our results show *V. parahaemolyticus* thrived alongside the phytoplankton in the experimental containers over the 60h period, suggesting *V. parahaemolyticus* may use ambient DOC produced by phytoplankton and other sources in coastal environments.

Virulent strains of *V. parahaemolyticus* produce either Type 3 secretion systems, which result in host cytotoxicity or enterotoxicity, or Type 6 secretion

systems, which can harm the host's intracellular transport methods (Ceccarelli et al. 2013). As suggested earlier, *V. parahaemolyticus* classified as "nonvirulent" still cause harm via processes we have not yet identified (Su & Liu 2007). In multicellular organisms such as humans and nematodes, nonvirulent *V. parahaemolyticus* causes strong inflammatory responses in effected organs (Ottaviani et al. 2012; Perez-Reytor & Garcia 2017). While mechanisms of the impact of *V. parahaemolyticus* on phytoplankton have not been identified, there are many studies on other harmful bacteria and their impact on phytoplankton communities. For example, some bacteria release quorum sensing molecules such as 2-heptyl-4-quinolone (HHQ), which can decrease the cellular division rate of phytoplankton (Pollara et al. 2021). Close relatives of *V. parahaemolyticus* such as *Vibrio cholerae* and *Vibrio harveyi* commonly engage in quorum sensing, but mechanisms of quorum sensing in *V. parahaemolyticus* have not yet been identified (Ng & Bassler 2009; Gode-Potratz & McCarter 2011).

The quantum efficiency (F_v/F_m) findings (Fig. A.2) were somewhat surprising. We had expected the samples containing *V. parahaemolyticus* to have lower quantum efficiency because we expected the bacteria to negatively impact the phytoplankton community due to previous studies and research on related bacteria (Klein et al. 2019). Typically, the F_v/F_m decreases as the average health of the phytoplankton community decreases. However, the presence of *V. parahaemolyticus* did not appear to have a significant impact on the average photosystem efficiency of the phytoplankton community. The absence of an

impact on F_v/F_m suggests *V. parahaemolyticus* may not negatively impact phytoplankton physiology. It is additionally surprising how high the F_v/F_m values were; the average F_v/F_m for the W group was 0.6830 and for the WV group was 0.68500 (Figure A.2). The theoretical maximum value of F_v/F_m is approximately 0.8 (Giannini & Ciotti 2016). Our F_v/F_m values were therefore high, indicating a very healthy phytoplankton community during our bioassays.

Photopigment concentrations are directly related to the abundance of certain phytoplankton groups (Mackey et al. 1996). The chl-*a* concentration represents total phytoplankton abundance in the community. The samples containing *V. parahaemolyticus* had a significantly lower concentration of chl-*a* than the control samples, with sample means of 20.7400 ug chl-*a* l^{-1} for the W group and 14.4080 ug chl-*a* l^{-1} for the WV group (Fig. A.3, Table A.2). This difference suggests there is lower total phytoplankton abundance in the presence of *V. parahaemolyticus*. These results support the previous findings of Klein et al. (2019) where *V. parahaemolyticus* decreased the chl-*a* fluorescence in monocultures of various phytoplankton. The exact mechanism by which "nontoxic" *V. parahaemolyticus* results in a decrease in total algal biomass is unknown.

There were also significantly lower concentrations of fucoxanthin, alloxanthin, and zeaxanthin in the samples with *V. parahaemolyticus* (Fig. A.3, Table A.2). This data, along with the ChemTax analysis, reveals there was a significant decrease in the abundances of diatoms, cryptophytes, and

cyanobacteria (Table 3.1). There was no significant difference in the abundances of dinoflagellates or green algae. Overall, there was a significant change in the overall phytoplankton community composition.

These results differ somewhat from previous experiments. In experiments with monocultures of coccolithophores, diatoms, and dinoflagellates, there were decreases in chl-*a* fluorescence (an indicator of biomass) in response to *V. parahaemolyticus* (Klein et al. 2019). In our experiments, there were no coccolithophores present (Fig. 3.1). The estimated abundance of diatoms did decrease, which aligns with the experiments of Klein et al. (2019). However, in our experiments, the estimated abundance of dinoflagellates did not significantly decrease with the *V. parahaemolyticus* exposure (Fig. 3.1). This difference in results supports the idea that microbes may respond to stressors differently when in the presence of other microbes (Amin et al. 2015; Filho et al. 2021). Further research would need to be done to identify why the dinoflagellates may have responded differently in our experiments than in the monoculture experiments.

Different types of phytoplankton have different responses to stress in their environments. For example, smaller phytoplankton, such as cyanobacteria, tend to do well in nutrient-deficient waters due to their high surface area-to-volume ratio (Van de Waal & Litchman 2020). However, larger species of phytoplankton, such as diatoms, perform well in waters with a high pCO_2 concentration due to the lower rate of diffusion in larger cells. In response to polycyclic aromatic hydrocarbons (PAHs), a toxin in crude oil, the small phytoplankton have the

greatest decrease in abundance (Echeveste et al. 2011). The presence of PAHs in various concentrations also results in a significant decrease in phytoplankton diversity (Huang et al. 2009) but not complete extinction, which suggests some species of phytoplankton are better able to endure environmental stressors. It is therefore unsurprising that, despite the decrease in total chl-*a* (Fig. A.3), the abundance of some groups of phytoplankton (dinoflagellates and green algae, in our case) remained unaffected, while the other groups (diatoms, cryptophytes, and cyanobacteria) decreased in abundance (Fig. 3.1). The exact mechanisms by which dinoflagellates and green algae were more tolerant of the presence of *V. parahaemolyticus* need further experimentation to be discovered.

The presence of *V. parahaemolyticus* also decreased the relative abundances of Proteobacteria, Actinobacteriota, Planctomycetota, Verrucomicrobiota, SAR 324, Chloroflexi, Myxococcota, Fibrobacterota, Nanoarchaeota, and NB1-j (Figure 3.2, Table 3.2). It also increased the relative abundance of Dependentiae. The Proteobacteria phylum is extremely diverse and serves many different purposes in marine environments, including processing complex molecules such as glycolate and metabolizing sulfur compounds (Gonzalez et al. 1999; Schada von Borzyskowski et al. 2019). Actinobacteriota is one of the most common phyla in coastal waters and its members are important to the C mineralization process (Miksch et al. 2021; Cai et al. 2022). The Planctomycetota phylum is important in both the C and N cycles (Vitorino et al. 2024). The Verrucomicrobiota group, in addition to contributing to cycling, is

responsible for breaking down complex molecules called fucose-containing sulfated polysaccharides (Orellana et al. 2022). SAR 324 is an extremely diverse phylum important to many marine ecosystems (Bouef et al. 2017; Malfertheiner et al. 2022). Chloroflexi is important in sediments for particle breakdown (Hug et al. 2013). Members of Myxococcota are photosynthetic and therefore contribute to global C cycling (Li et al. 2023). Fibrobacterota species are important for breaking down cellulose, particularly in estuarine sediments (Yu et al. 2023). Nanoarchaeota is a relatively recently discovered phylum and is not yet well understood (Huber et al. 2002). The NB1-J phylum contributes to nitrification (Voogd et al. 2015). Dependentiae, the only phylum that increased, has also been shown to increase with the addition of *V. parahaemolyticus* in studies on the clam microbiome (Wang et al. 2020). Members of the Dependentiae phylum have relatively small genomes and have parasitic lineages (Yeoh et al. 2015). In summary, the bacterial groups affected by the presence of *V. parahaemolyticus* are important in the ecosystem and serve a wide variety of functions.

It is also worth noting the relative abundance of *V. parahaemolyticus* decreased drastically over the course of the experiment (Fig. 3.4). At 0h, the order Vibrionales makes up approximately ninety percent (90%) of the prokaryotic community in the WV group; at 60h, Vibrionales makes up only approximately 7.5% of the prokaryotic community in the WV group. This drastic decrease in the relative abundance *V. parahaemolyticus* was not represented in the CFU data (Table A.1). The ability of the prokaryotic community to survive and

outcompete the *V. parahaemolyticus* population present is important to note. However, the absolute abundance of prokaryotic organisms was not measured in this experiment and we therefore cannot draw conclusions about the resilience of the prokaryotic community in response to this pathogen.

V. parahaemolyticus may soon increase in abundance in nature due to rising global temperatures and increasing coastal anthropogenic impacts (Su & Liu 2007). As bacterial concentrations increase, the risk of harm to the phytoplankton community increases too. Phytoplankton of all types are important to the entire ecosystem. In addition to serving as the base of most marine food chains, phytoplankton are responsible for 50% of the world's oxygen production (Litchman et al. 2015). Therefore, healthy phytoplankton communities are essential for the survival and health of all living things.

Our research suggests *V. parahaemolyticus* has a negative impact on phytoplankton biomass as well as an impact on phytoplankton and bacterial community compositions. While the change in community compositions cannot inherently be defined as "good" or "bad," any change in community composition impacts the functioning of the microbial community and ecosystem. It is impossible for us to know how exactly this change in function might have larger implications for ecosystem health without further studies. However, it is clear *V. parahaemolyticus* poses a real threat to the current phytoplankton assemblage in estuarine and coastal microbial communities.

The abundance of *V. parahaemolyticus* should be closely monitored and further research should be performed to better understand the full implications of the rising *V. parahaemolyticus* populations numbers. We also recommend altering seafood collection practices, especially during the summer months when phytoplankton (which many bivalves consume as their primary source of food) and *V. parahaemolyticus* are both at their highest abundances. Raising awareness about this pathogen in the seafood industry may decrease incidences of *V. parahaemolyticus* infections. These steps are essential to maintaining human and ecosystem health.

References

Aiken J, Pradhan Y, Barlow R, Lavender S, Poulton P, Holligan P, & Hardman-Mountford N. 2009. Phytoplankton pigments and functional types in the Atlantic Ocean: a decadal assessment, 1995-2005. Deep Sea Research 56 (15): 899-917.

Amin SA, Hmelo LR, Van Tol HM, Durham BP, Carlson LT, Heal KR, et al. 2015. Interaction and signaling between a cosmopolitan phytoplankton and associated bacteria. Nature 522: 98-101.

Baker-Austin C, Stockley L, Rangdale R, Martinez-Urtaza J. 2010. Environmental Occurrence and Clinical Impact of *Vibrio vulnificus* and *Vibrio parahaemolyticus*: a European perspective. Environmental Microbiology Reports 2 (1): 7-18.

Beardall J, Young E, & Roberts S. 2001. Approaches for determining phytoplankton nutrient limitation. Aquatic Sciences 63: 44-69.

Berman-Frank I, Lundgren P, & Falkowski P. 2003. Nitrogen fixation and photosynthetic oxygen evolution in cyanobacteria. Research in Microbiology 154 (3): 157-64.

Bouef D, Eppley JM, Mende DR, Malmstrom RR, Woyke T, DeLong EF. 2021. Metapangenomics reveals depth-dependent shifts in metabolic potential for the ubiquitous marine bacterial SAR324 lineage. Microbiome 9 (172).

Brumfield KD, Chen AJ, Gangwar M, Usmani M, Hasan NA, Jutla AS, et al. 2023. Environmental Factors Influencing Occurrence of *Vibrio parahaemolyticus* and *Vibrio vulnificus*. Applied and Environmental Microbiology 89 (6).

Cai S, Wang F, Laws EA, Liu Y, Xu C, Ma L, et al. 2022. Linkages between bacterial community and extracellular enzyme activities crossing a coastal front. Ecological Indicators 145.

Camarena-Gomez MT, Lipsewers T, Piiparinen J, Eronen-Rasimus E, Perez-Quemalinos D, Hoikkala L, et al. 2018. Shifts in phytoplankton community structure modify bacterial production, abundance and community composition. Aquatic Microbial Ecology 81: 149-70.

Ceccarelli D, Hasan NA, Huq A, & Colwell RR. 2013. Distribution and dynamics of epidemic and pandemic *Vibrio parahaemolyticus* virulence factors. Frontiers in Cellular and Infection Microbiology 3.

Correa Velez KE, Leighton RE, Decho AW, Pinckney JL, & Norman RS. 2023. Modeling pH and temperature effects as climatic hazards in *Vibrio vulnificus* and *Vibrio parahaemolyticus* planktonic growth and biofilm formation. GeoHealth 7.

Crump BC & Bowen JL. 2024. The microbial ecology of estuarine ecosystems. Annual Review of Marine Science 16: 335-60.

Drake SL, DePaola A, & Jaykus L. 2007. An Overview of *Vibrio vulnificus* and *Vibrio parahaemolyticus*. Comprehensive Reviews in Food Science and Safety 6 (4): 120-44.

Filho MMB, Walker M, Ashworth MP, & Morris JJ. 2021. Structure and Long-Term Stability of the Microbiome in Diverse Diatom Cultures. Microbiol Spectr 9 (1).

Flores E & Herrero A. 2005. Nitrogen assimilation and nitrogen control in cyanobacteria. Biochemical Society Transactions 33 (1): 164-7.

Giannini MFC & Ciotti AM. 2016. Parameterization of natural phytoplankton photo-physiology: Effects of cell size and nutrient concentration. Limnology and Oceanography 61 (4): 1495-512.

Gode-Potratz CJ & McCarter LL. 2011. Quorum sensing and silencing in *Vibrio parahaemolyticus.* Journal of Bacteriology 193 (16).

Gonzalez JM, Kiene RP, Moran MA. 1999. Transformation of sulfur compounds by an abundant lineage of marine bacteria in the α-subclass of the class *Proteobacteria*. Applied and Environmental Microbiology 65 (9).

Heil CA, Revilla M, Gilbert PM, & Murasko S. 2007. Nutrient quality drives differential phytoplankton community composition on the southwest Florida shelf. Limnology and Oceanography 52 (3): 1067-78.

Higgins H, Wright S, & Schlüter L. Quantitative interpretation of chemotaxonomic pigment data. In: Roy S, Llewellyn CA, Egeland ES, & Johnsen G. Phytoplankton pigments. New York: Cambridge University Press; 2011. 257-313.

Huang Y, Jiang Z, Zeng J, Chen Q, Zhao Y, Liao Y, Shou L, & Xu X. 2011. The chronic effects of oil pollution on marine phytoplankton in a subtropical bay, China. Environmental Monitoring Assessment 176: 517-30.

Huber H, Hohn MJ, Rachel R, Fuchs T, Wimmer VC, & Stetter KO. 2002. A new phylum of Archaea represented by a nanosized hypothermophilic symbiont. Nature 417: 63-7.

Hug LA, Castelle CJ, Wrighton KC, Thomas BC, Sharon I, Frischkorn KR, et al. 2013. Community genomic analyses constrain the distribution of metabolic traits across the Chloroflexi phylum and indicate roles in sediment carbon cycling. Microbiome 1 (22).

Klein SL, Haney KE, Hornaday TM, Gartmon IB, & Lovell CR. 2019. Interactions between the human pathogen *Vibrio parahaemolyticus* and common marine microalgae. Common Trends in Microbiology 145.

Li L, Huang D, Hu Y, Rudling NM, Canniffe DP, Wang F, et al. 2023. Globally distributed *Myxococcota* with photosynthesis gene clusters illuminate the origin and evolution of a potentially chimeric lifestyle. Nature Communications 14 (6450).

Litchman E, de Tezanos Pinto P, Edwards KF, Klausmeier CA, Kremer CT, Thomas MK. 2015. Global biogeochemical impacts of phytoplankton: a trait-based perspective. Journal of Ecology 103 (6): 1384-1396.

Logue JB, Stedmon CA, Kellerman AM, Nielson NJ, Andersson AF, Laudon H, et al. 2016. Experimental insights into the importance of aquatic bacterial community composition to the degradation of dissolved organic matter. The ISME Journal 10 (3): 533-45.

Mackey MD, Mackey DJ, Higgins HW, & Wright SW. 1996. CHEMTAX – a program for estimating class abundances from chemical markers: application to HPLC measurements of phytoplankton. Marine Ecology Progress Series 144: 265-83.

Main CR, Salvitti LR, Whereat EB, & Coyne KJ. 2015. Community-Level and Species-Specific Associations between Phytoplankton and Particle-Associated Vibrio Species in Delaware's Inland Bays. Applied and Environmental Microbiology 81 (17).

Malfertheiner L, Martinez-Perez C, Zhao Z, Herndl GJ, Baltar F. 2022. Phylogeny and metabolic potential of the candidate phylum SAR324. Biology 11 (4): 599.

Matsuda S, Hiyoshi H, Tandhavanant S, & Kodama T. 2019. Advances on *Vibrio parahaemolyticus* research in the postgenomic era. Microbiology and Immunology 64 (3): 167-81.

Miksch S, Meiners M, Meyerdierks A, Probandt D, Wegener G, Titschack J, et al. 2021. Bacterial communities in temperate and polar coastal sands are seasonally stable. ISME Communications 1 (29).

Millie DF, Schofield OME, Kirkpatrick GJ, Johnsen G, & Evens TJ. 2002. Using absorbance and fluorescence spectra to discriminate microalgae. European Journal of Phycology 37 (3).

Ng W & Bassler BL. 2009. Bacterial quorum-sensing network architectures. Annual Review of Genetics 43: 197-222.

Orellana LH, Francis TB, Ferraro M, Hehemann J, Fuchs BM, & Amann RI. 2021. *Verrucomicrobiota* are specialist consumers of sulfated methyl pentoses during diatom blooms. The ISME Journal 16: 630-41.

Ottiaviani D, Leoni F, Serra R, Serracca L, Decastelli L, Rocchegiani E, et al. 2012. Nontoxigenic *Vibrio parahaemolyticus* strains causing acute gastroenteritis. Journal of Clinical Microbiology 50 (12).

Pan X, Mannino A, Marshall HG, Filippino KC, & Mullholland MR. 2011. Remote sensing of phytoplankton community composition along the northeastern coast of the United States. Remote Sensing of Environment 115 (12): 3731-47.

Perez-Reytor D & Garcia K. 2017. *Galleria mellonella*: A model of infection to discern novel mechanisms of pathogenesis of non-toxigenic *Vibrio parahaemolyticus* strains. Virulence 9 (1): 22-24.

Pinckney J, Millie D, Howe K, Paerl H, & Hurley J. 1996. Flow scintillation counting of 14C-labeled microalgal photosynthetic pigments. Journal of Plankton Research 18: 1867–1880.

Pinckney J, Richardson T, Millie D, Paerl H. 2001. Application of photopigment biomarkers for quantifying microalgal community composition and *in situ* growth rates. Organic Geochemistry 32: 585–595.

Pollara SB, Becker JW, Nunn BL, Boiteau R, Repeta D, Mudge MC, et al. 2021. Bacterial quorum-sensing signal arrests phytoplankton cell division and impacts virus-induced mortality. Environmental Microbiology 6 (3).

Rath KM, Fierer N, Murphy DV, & Rousk J. 2019. Linking bacterial community composition to soil salinity along environmental gradients. The ISME Journal 13 (3): 836-46.

Rosales D, Ellet A, Jacobs J, Ozbay G, Parveen S, & Pitula J. 2022. Investigating the Relationship between Nitrate, Total Dissolved Nitrogen, and Phosphate

with Abundance of Pathogenic Vibrios and Harmful Algal Blooms in Rehoboth Bay, Delaware. Applied and Environmental Microbiology 88 (14).

Salomon D, Gonzalez H, Updegraff BL, & Orth K. 2013. *Vibrio parahaemolyticus* Type VI Secretion System 1 is activated in marine conditions to target bacteria, and is differentially regulated from System 2. PLoS ONE 8 (4).

Schada von Borzyskowski L, Severi F, Kruger K, Hermann L, Gilardet A, Sippel F, et al. 2019. Marine Proteobacteria metabolize glycolate via the β-hydroxyaspartate cycle. Nature 575: 500-4.

Su YC & Liu C. 2007. *Vibrio parahaemolyticus*: A concern of seafood safety. Food Microbiology 24 (6): 549-558.

Sun Z, Li G, Wang C, Jing Y, Zhu Y, Zhang S, et al. 2014. Community dynamics of prokaryotic and eukaryotic microbes in an estuary reservoir. Scientific Reports 4.

Van de Waal DB & Litchman E. 2020. Multiple global change stressor effects on phytoplankton nutrient acquisition in a future ocean. Philos Trans R Soc Lond B Biol Sci 375 (1798).

Vitorino IR, Pinto E, Martin J, Mackenzie TA, Ramos MC, Sanchez P, et al. 2024. Uncovering the biotechnological capacity of marine and brackish water *Planctomycetota*. Antonie van Leeuwenhoek 117 (26).

Voogd NJ, Cleary DFR, Polonia ARM, & Gomes NCM. 2015. Bacterial community composition and predicted functional ecology of sponges, sediment and seawater from the thousand islands reef complex, West Java, Indonesia. Microbiology Ecology 91 (4).

Wang H, Yue X, Yu J, Wang R, Teng S, Fang J, et al. 2020. Microbial community changes in the digestive tract of the clam *Meretrix petechialis* in response to *Vibrio parahaemolyticus* challenge. Journal of Oceanology and Limnology 39: 329-39.

Weissbach A, Rustrom M, Olofsson M, Bechemin C, Icely J, Newton A, et al. 2011. Phytoplankton allelochemical interactions change microbial food web dynamics. Limnology & Oceanography 56 (3): 899-909.

Yentsch CS & Phinney DA. 1985. Spectral fluorescence: an ataxonomic tool for studying the structure of phytoplankton populations. Journal of Phytoplankton Research 7 (5): 617-32.

Yeoh YK, Sekiguchi Y, Parks DH, & Hugenholtz P. 2016. Comparative genomics of candidate phylum TM6 suggests that parasitism is widespread and ancestral in this lineage. Molecular Biology and Evolution 33 (4): 915-27.

Yu T, Wu W, Liang W, Wang Y, Hou J, Chen Y, et al. 2023. Anaerobic degradation of organic carbon supports uncultured microbial populations in estuarine sediments. Microbiome 11 (81).

Appendix A: Supplemental Figures

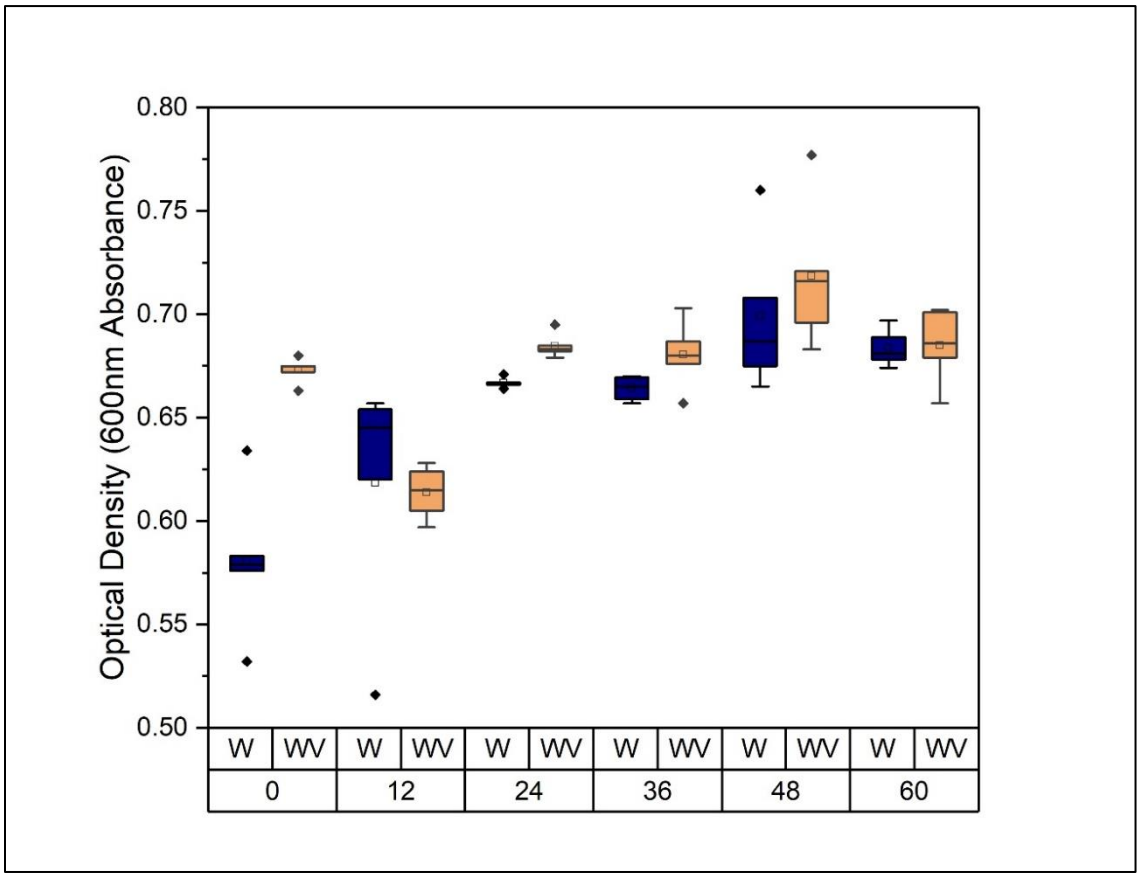

Figure A.1. The optical density (indicative of cell concentration) at each time point for each experimental condition. WV and W denote with and without *V. parahaemolyticus* added, respectively. Time points for the measurements are given on the x-axis. The boxplot indicates the first and third quartiles and the whiskers show 5 and 95% confidence intervals. Outliers are indicated by symbols.

Table A.1. The CFU counts of *V. parahaemolyticus* at each time point

		D1		D2		D3	D4
Hour	**Replicate**	**W**	**WV**	**W**	**WV**	**WV**	**WV**
0	1	0	TNTC	--	--	--	--
	2	0	TNTC	--	--	--	--
	3	0	TNTC	--	--	--	--
12	1	0	TNTC	--	TNTC	400	--
	2	0	TNTC	--	TNTC	400	--
	3	0	TNTC	--	TNTC	320	--
24	1	0	TNTC	--	TNTC	1752	--
	2	15	TNTC	--	TNTC	1652	--
	3	0	TNTC	--	TNTC	TNTC	--
48	1	2	--	--	--	34	6
	2	0	--	--	--	167	436
	3	1	--	--	--	1012	114
60	1	0	--	--	--	TNTC	0
	2	0	--	--	--	TNTC	TNTC
	3	0	--	--	--	TNTC	TNTC

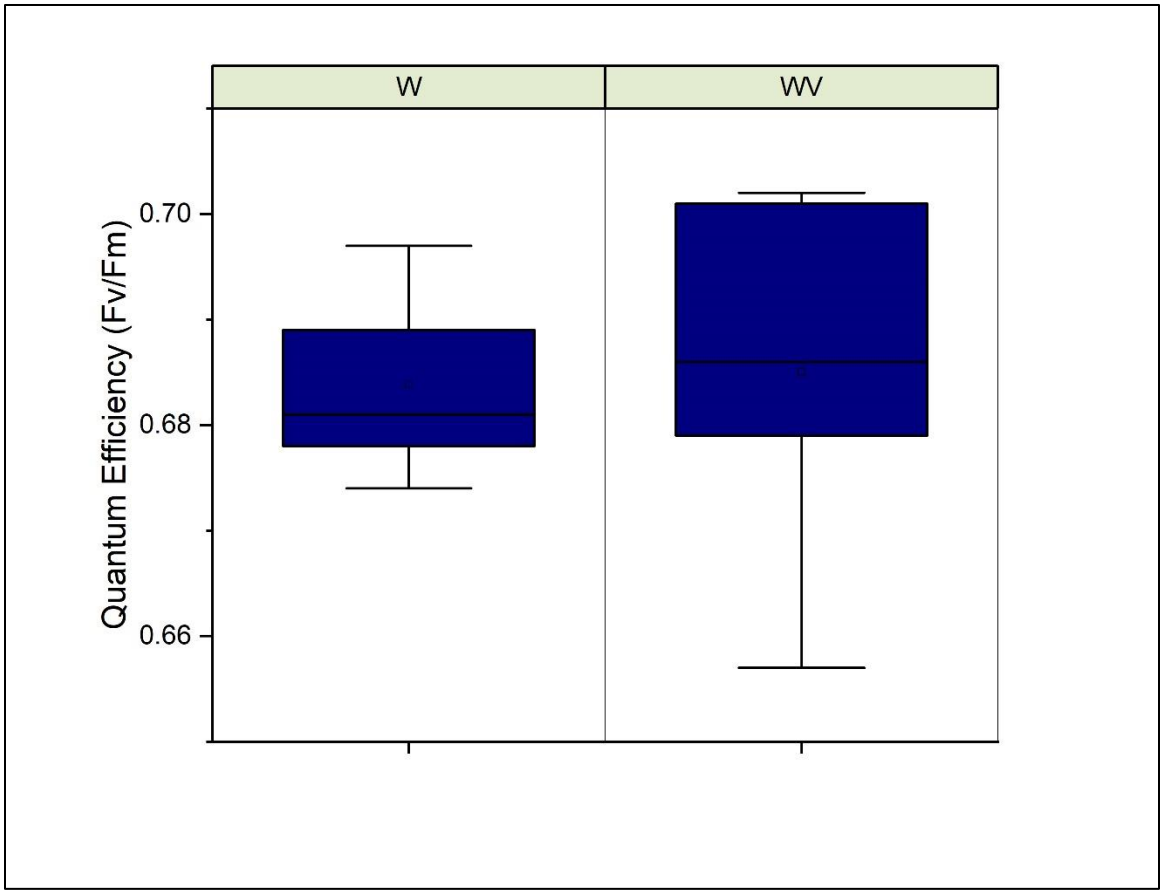

Figure A.2. The quantum efficiency (F_v/F_m) of each experimental condition at 60h. WV and W denote with and without *V. parahaemolyticus* added, respectively. The boxplot indicates the first and third quartiles and the whiskers show 5 and 95% confidence intervals. Outliers are indicated by symbols. W: $\bar{x}$ = 0.6830 ± 0.009203. WV: $\bar{x}$ = 0.68500 ± 0.018480.

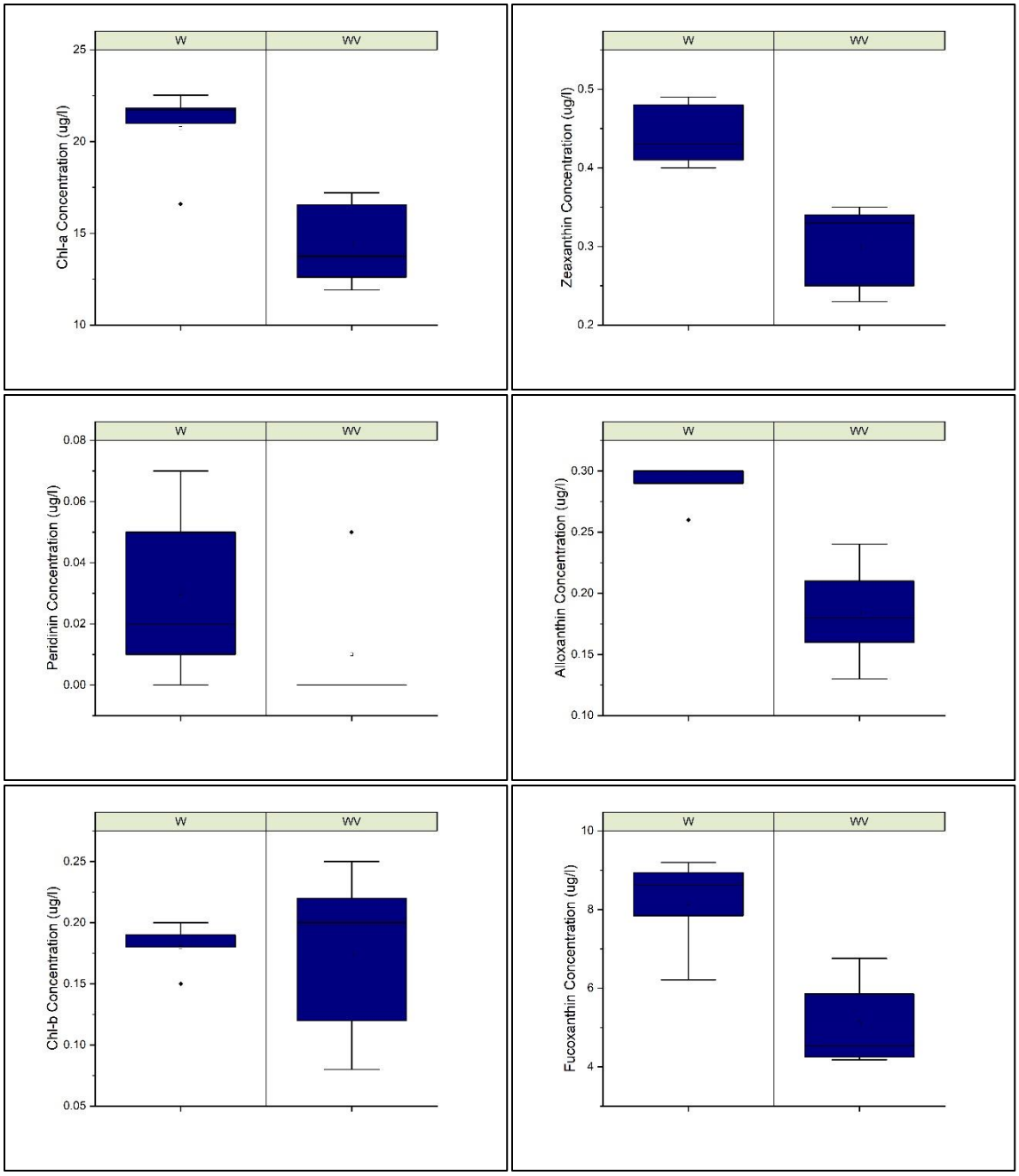

Figure A.3. The concentrations of chl-*a*, zeaxanthin, peridinin, chl-*b*, alloxanthin, and fucoxanthin at 60h for both experimental conditions in units of ug l^{-1}. WV and W denote with and without *V. parahaemolyticus* added, respectively. Time points for the measurements are given on the x-axis. The boxplot indicates the first and third quartiles and the whiskers show 5 and 95% confidence intervals. Outliers are indicated by symbols.

Table A.2. MANOVA results with sample means and standard deviations for photopigment concentrations at 60h

Photopigment	**$F_{1,8}$**	**P-value**	**W $\bar{x}$ ± SD**	**WV $\bar{x}$ ± SD**
Chl-*a*	17.854	0.003*	20.7400 ± 2.37790	14.4080 ± 2.36089
Zeaxanthin	21.136	0.002*	0.4420 ± 0.04087	0.3000 ± 0.05568
Peridinin	1.481	0.258	0.0300 ± 0.02915	0.0100 ± 0.02236
Chl-*b*	0.033	0.860	0.1800 ± 0.01871	0.1740 ± 0.07127
Alloxanthin	23.579	0.001*	0.2960 ± 0.02881	0.1840 ± 0.04278
Fucoxanthin	16.865	0.003*	8.1620 ± 1.20483	5.1140 ± 1.14137

Appendix B: Supplemental Methods

Table B.1 Seawater media components

Component	**Quantity added**
Salt water base	100 ml
MOPS	1 ml
NH_4Cl	1 ml
PO_4^-	1 ml
Trace metals	0.1 ml
Yeast extract	0.25 g
Peptone	0.25g